

Exfoliation of graphene oxide and its application in improving the electro-optical response of ferroelectric liquid crystal

Veeresh Kumar, Ajay Kumar, Shruti Bhandari, A. M. Biradar, G. B. Reddy, and Renu Pasricha

Citation: [Journal of Applied Physics](#) **118**, 114904 (2015); doi: 10.1063/1.4930949

View online: <http://dx.doi.org/10.1063/1.4930949>

View Table of Contents: <http://scitation.aip.org/content/aip/journal/jap/118/11?ver=pdfcov>

Published by the [AIP Publishing](#)

Articles you may be interested in

[Effects of graphene on electro-optic switching and spontaneous polarization of a ferroelectric liquid crystal](#)
Appl. Phys. Lett. **105**, 112905 (2014); 10.1063/1.4896112

[Copper oxide decorated multi-walled carbon nanotubes/ferroelectric liquid crystal composites for faster display devices](#)
J. Appl. Phys. **112**, 054309 (2012); 10.1063/1.4748958

[Dielectric and electro-optical studies of glycerol/ferroelectric liquid crystal mixture at room temperature](#)
J. Appl. Phys. **105**, 124101 (2009); 10.1063/1.3149781

[V-shaped electro-optic response observed in a chiral ferroelectric smectic liquid crystal](#)
Appl. Phys. Lett. **93**, 093507 (2008); 10.1063/1.2970039

[Charge controlled, fixed optic axis analog \("v-shaped"\) switching of a bent-core ferroelectric liquid crystal](#)
Appl. Phys. Lett. **85**, 6344 (2004); 10.1063/1.1842372

The logo for AIP APL Photonics is displayed. It features the letters 'AIP' in a large, white, sans-serif font, followed by a vertical orange bar and the words 'APL Photonics' in a smaller, white, sans-serif font. The background is a dark red with a subtle, swirling pattern.

APL Photonics is pleased to announce
Benjamin Eggleton as its Editor-in-Chief



Exfoliation of graphene oxide and its application in improving the electro-optical response of ferroelectric liquid crystal

Veeresh Kumar,^{1,2} Ajay Kumar,³ Shruti Bhandari,¹ A. M. Biradar,¹ G. B. Reddy,² and Renu Pasricha^{1,a)}

¹CSIR-National Physical Laboratory, Dr K S Krishnan Road, New Delhi 110012, India

²Department of Physics, Indian Institute of Technology, New Delhi 110016, India

³Department of Physics, Deshbandhu College, University of Delhi, Delhi 110019, India

(Received 15 June 2015; accepted 1 September 2015; published online 16 September 2015)

Near complete exfoliation and reduction of lyophilized graphene oxide (GO) has been carried out at temperature as low as 400 °C. The structural characterizations of the reduced GO have been performed using X-ray diffraction, Fourier transform infrared spectroscopy, and Raman spectroscopy techniques. The morphological studies were carried out using scanning electron microscopy. The synthesized GO finds an application in improving the switching performance of a liquid crystal (LC) mixture by remarkably modifying the physical properties, such as spontaneous polarization and rotational viscosity of the ferroelectric LC (FLC) material which in turn resulted into faster response of the FLC. The present study explores the possibility of low temperature thermal reduction of GO along with its application in improving the properties of LC based display systems. © 2015 AIP Publishing LLC. [<http://dx.doi.org/10.1063/1.4930949>]

I. INTRODUCTION

In recent years, graphene has attracted a great deal of attention of researchers for its promising technological applications.^{1,2} Graphene is a two dimensional (2D) material in which the dynamics of conduction electrons is described by the Dirac equation rather than the usual Schrödinger's equation.³ It has been utilized as the building block of promising materials with different dimensions ranging from fullerene to graphite.² Various methods, such as chemical vapor deposition (CVD), mechanical exfoliation of graphite (i.e., process of transforming stacked layers of graphite into single layer graphene), and reduction (chemical/thermal) of graphene oxide (GO) have been introduced to synthesize graphene.⁴⁻⁶ Among the above said methods, the presence of residual oxygen in the form of functional groups has limited the synthesis of GO by chemical reduction processes.⁷ This residual oxygen reduces the electron density at the Fermi level and, at the same time, may change the hybridization from planar sp^2 to tetrahedral sp^3 which in turn lowers the conductivity of graphene.^{8,9} Thermal reduction, on the other hand, produces graphene with less agglomeration, higher electrical conductivity, and specific surface area.¹⁰ However, requirement of higher temperatures (>1000 °C) and sophisticated environment to restrict carbon loss (or decomposition) has been the limiting factor of this method.^{11,12} In view of a recent report proposing the possibility of complete exfoliation of GO at lower temperatures,⁹ various research groups have motivated to explore the routes for synthesis of graphene at lower temperatures. Wan *et al.* have reported the thermal reduction of GO sheets dispersed in N, N-dimethylacetamide (DMAc) and water (10: 3 v/v) at 150 °C

under the protection of nitrogen gas.¹³ Vacuum assisted synthesis of few layered graphene by thermally reducing GO at 135 °C and their subsequent use in improving the conductivity of polymers have also been reported.¹⁴ Zhang *et al.* synthesized graphene sheets at 200 °C, under negative pressure environment which showed excellent energy storage performance.¹⁵ However, use of suitable chemicals, controlled vacuum environment, and long annealing time is found to be some crucial requirements in above mentioned methods. In the present paper, we demonstrated a step wise low temperature exfoliation and reduction of lyophilized GO. We carried out systematic thermal reduction of graphite oxide and investigated the effect of temperature and abridging oxygen on the structure of GO sheets. We increased the reduction temperature in steps and found that no structural changes took place beyond 500 °C.

Recently, graphene based nanostructures have shown promising effects on the electro-optical properties of liquid crystal (LC) materials. Lv *et al.* have observed that the presence of GO can induce uniform vertical alignment of ferroelectric LCs (FLCs) and modified the dielectric relaxation process remarkably.¹⁶ We investigated the effect of graphene quantum dots on the display characteristics of FLC material and observed the improved electro-optical response and photoluminescence emission.¹⁷ In view of the above results, we dispersed the synthesized GO annealed at different temperatures into the FLC material FLC W301 and analyzed the effect of the same on the dielectric and electro-optical properties of the later. We found the GO dispersed FLC mixtures possess faster switching process in comparison to that of pure FLC material.

II. EXPERIMENTAL

The aqueous solution of GO was prepared from natural graphite powder by modified Hummer's method.¹⁸ GO was

^{a)} Author to whom correspondence should be addressed. Electronic addresses: renup@ncbs.res.in and renu1505@gmail.com. Phone: +91-80-2366-6390; Fax: +91-80-23666396. Present address: NCBS-TIFR, Bangalore, India.

prepared from natural graphite powder (Alfa assar 99.999%). In a typical reaction, 1 g of graphite with 1 g of NaNO_3 was mixed in 46 ml of H_2SO_4 and stirred in an ice bath followed by slow addition of 6 g KMnO_4 . The obtained solution was transferred to a $35 \pm 5^\circ\text{C}$ water bath for stirring till a thick paste is formed. 90 ml of water was added to the obtained paste and the solution was again stirred for 30 min while the temperature was raised to $90 \pm 5^\circ\text{C}$. Finally, 200 ml of water was added, followed by the slow addition of 3 ml of H_2O_2 (30%), the color of the solution turned from dark brown to yellow. The warm solution was then filtered and washed with 200 ml of water. The filter cake was then dispersed in water by mechanical agitation. To separate out the thicker GO flakes, the solution was centrifuged 3–4 times at low rpm for 2–2 min. The supernatant then underwent two more high-speed centrifugation steps to remove small GO pieces. The prepared GO was dried by lyophilization process and recovered powder was collected and stored at room temperature in a desiccators. GO was annealed in stages, starting from 100°C and proceeding in steps of 100°C to reach 500°C . The nomenclature for samples obtained after each step is given as GO (as prepared) and GO-100, GO-200, GO-300, GO-400, and GO-500, respectively.

The FLC material, namely, FLC W301 is used for the present study. The dielectric and electro-optical characterization of FLC W301 has been reported earlier.¹⁹ To disperse GO into the FLC material, the suspension of GO in DI water was obtained by ultrasonication of the suspension for 1 h. For GO/FLC mixtures, the suitable amount of GO suspension was added into the appropriate amount of FLC material using micro-pipette and was uniformly mixed. The resulting mixture was then placed in the oven at temperature well above the boiling point of water for 10 min and then taken out, again mixed, and placed in the oven. This process was repeated for 3–4 times to ensure the complete evaporation of DI water from FLC. Conducting indium tin oxide (ITO) coated glass plates were used to fabricate LC sample cells. The desired (squared) electrode pattern ($0.45 \times 0.45 \text{ cm}^2$) of ITO on the glass plates was achieved using photolithography technique. Conventional rubbed polyimide technique is used for the homogeneous alignment of FLC cells. The thickness of the sample cells is maintained around $\sim 7 \mu\text{m}$ using Mylar spacers. The samples (pure and GO doped) were filled into the sample cells by capillary action above the isotropic temperature of the material. The optical micrographs of pure and GO doped FLC material were recorded using a polarizing optical microscope (Ax-40, Carl Zeiss, Germany) fitted with a charge-coupled device camera and interfaced with a computer. The dielectric measurements were carried out by using an impedance analyzer (Wayne Kerr, 6540 A, UK) in the frequency range 20 Hz–1 MHz with measuring voltage of 0.5 V_{pp} . The material parameters of pure and GO doped FLC W301 are measured with the help of Automatic liquid crystal tester, ALCT-P, Instec, USA. One may directly determine the values of material parameters by fixing the sample cell parameters through the software. The ALCT-P evaluates the P_s value by applying an alternating electric field (triangular waveform) having certain frequency across the sample cell and is based on triangular wave pulse method.²⁰ It also

directly gives the value of rotational viscosity of the sample along with that of P_s .

III. RESULTS AND DISCUSSION

It was observed from the scanning electron microscopy (SEM) images that the prepared sheets were of large size. For SEM images of GO and finally reduced GO, see supplementary material, Figure S1.³⁶ The change in the interlayer spacing (d_{002}) of annealed GO with increase in temperature (i.e., from room temperature to 500°C) was analyzed by X-ray diffraction (XRD) [Figure 1(a)]. The d_{002} value of bulk graphite used in our experiment was 3.35 \AA ($2\theta \approx 26.54^\circ$), calculated by Bragg's law. The XRD of graphite, Figure S2 is given in the supplementary material.³⁶ It has been observed that the shape of graphite particles was maintained upon oxidation from graphite to GO. However, a remarkable increase in the direction of C-axis was observed due to the presence of oxygen containing functional groups and d_{002} values were found to increase from 3.35 to 8.42 \AA ($2\theta \approx 10.5^\circ$) for lyophilized GO. With further increase in the annealing temperature, the (d_{002}) peak of GO was shifted to the higher 2θ values [8.11 \AA ($2\theta = 10.9^\circ$) for GO-100]. At 200°C , no peak was observed in the XRD pattern that could be due to the drastic vaporization of H_2O molecules. Above 300°C , lattice relaxation took place and we observed a broad peak centered at $2\theta = 26.18^\circ$ with the corresponding d_{002} value at 3.40 \AA in the XRD pattern at 400°C [Figure 1(a)]. On further increasing the temperature to 500°C , the XRD pattern was appeared to be the same as that of 400°C .

The Fourier transform infrared spectroscopy (FTIR) study was performed to study the extent oxygen moieties and thus it indicates the steady removal of oxygen containing groups from GO with increase in the reduction temperature. Figure 1(b) represents the FTIR spectra of GO and the subsequent products on step wise annealing. Graphite shows the carbon backbone ($\text{C}=\text{C}$) stretching at 1562 cm^{-1} and the peak at 1723 cm^{-1} relates to the stretching vibrations of carbonyl and carboxyl ($\text{C}=\text{O}$) groups adjacent to benzene rings.^{21,22} The epoxy ($\text{C}-\text{O}-\text{C}$) stretching and alkoxy ($\text{C}-\text{O}$) stretching vibrations are observed at 1222 cm^{-1} and 1050 cm^{-1} , respectively.²² As the reducing temperature was taken to higher value, the groups present at 1620 cm^{-1} disappeared and new peak at 1580 cm^{-1} related to $\text{C}=\text{C}$ vibrations emerged along with $\text{C}-\text{O}$ stretching vibrations peak at 1230 cm^{-1} . There was complete elimination of hydroxyl groups at and above 200°C . Since CO is strong reducing agent therefore formation of CO is highly expected. However, the mechanism of CO formation in thermal reduction is not well known.²³ At 200°C , the possibility of attacking hydroxyl radicals with CO is responsible for maximum CO_2 production. At 400°C and 500°C , no remarkable variation in the intensity of $\text{C}=\text{C}$ band was found. This can be understood that most of the functional groups had been removed at 400°C temperature giving a structure containing large sp^2 domains.

Raman spectroscopy was used to measure significant structural changes during the reduction process. The main feature in Raman spectra of GO is the D and G bands. The G

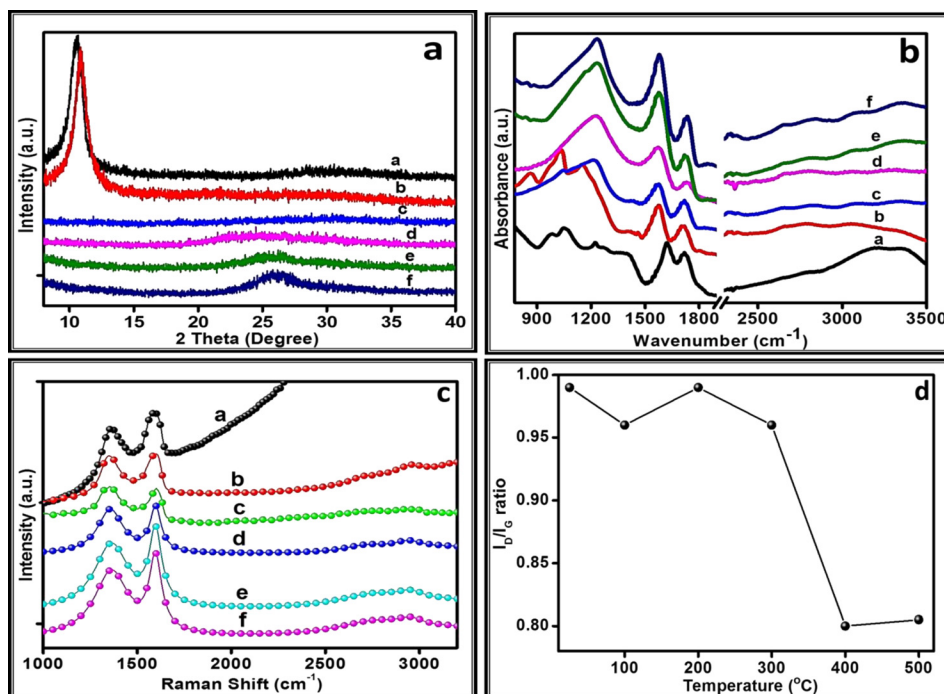


FIG. 1. (a) XRD pattern, (b) FTIR spectra, (c) Raman spectra, and (d) variation of I_D/I_G ratio of GO and annealed GO at different temperatures (100 °C, 200 °C, 300 °C, 400 °C, and 500 °C are marked as (a)–(f), respectively).

peak corresponds to the high frequency phonon (E_{2g}) at the center of Brillouin zone, while the D peak originates from breathing modes of six atom rings²⁴ and its activation requires defects, such as vacancies, amorphous carbon species. In other words, the D peak is the indication of disorders in graphene layers. The D and G band positions are indicated at 1350 cm^{-1} and 1580 cm^{-1} for graphitic structure, respectively.²⁵ Supplementary material, Figure S3, shows the Raman spectrum of graphite.³⁶ Figure 1(c) represents Raman spectra of GO recorded at different annealing temperatures and Figure 1(d) represents corresponding I_D/I_G ratio. A continuous increase in the intensity in GO sample may be attributed to the fact that GO has photoluminescence character. In the course of step wise increase in the temperature, we noticed a shift in G band towards high energy. The plausible reason for this behavior could be the blue shift of the G band as we go from bulk graphite to single layer of graphite, following the relation $\omega_G = 1581.6 + 11/(1 + n^{1.6})$, where ω_G is the frequency of G band.²⁶ Substrate effect may also be one of the reasons of this high energy shift.²⁷ See supplementary material for the full details of peak positions with Lorentz fitted curves, Figures S4–S6 and Table.³⁶ With increase in the annealing temperature, there was a decrease in the I_D/I_G ratio which clearly indicates an increase in the size of sp^2 cluster and the decrease in the degree of disorders, except a discrepancy at 200 °C. The intensity ratio was found to increase at annealing temperature 200 °C. This increase could be due to the defect formation because of fast removal of CO_2 . The I_D/I_G ratio is the measure of size of sp^2 clusters and the degree of disorders found in graphene. We found no change in the I_D/I_G ratio for GO-400 °C and GO-500 °C, which proves that most of the exfoliation and reduction took place at 400 °C which is in accordance with the XRD results.

As discussed, graphene based materials shown interesting effects on the physical properties of FLC materials, we dispersed GO and GO annealed at different temperatures to

observe the effect of the same on FLC material FLC W301. The pre-requisite condition for better performance for a LC composite is its alignment. We analyzed the alignment of GO doped FLC samples by observing their optical micrographs under the crossed polarizers. Different concentrations ranging from 0.05 wt. % to 0.2 wt. % of GO were mixed with the FLC material and the alignment of the resulting mixtures was analyzed. We found 0.1 wt. % of GO (to that of FLC W301) as the suitable amount that can be added to FLC material without any remarkable degradation of FLC alignment.

Figure 2 shows the dark and bright states of pure, 0.1 wt. % GO (as synthesized), GO-200, and GO-400 doped FLC W301 material. As can be seen from figure, the presence of GO has not degraded the alignment of the FLC material (especially bright states). However, leakage of light through major portions of the sample in the dark state is observed in case of 0.1 wt. % non-reduced GO doped FLC W301 [Figure 2(c)]. The presence of stripes in the dark states is due to the well known chevron defects of FLC materials.²⁸ It can also be clearly observed that such defects are present in pure and GO doped FLC W301 samples. However, the presence of such defects seems prominent in case of 0.1 wt. % GO (as synthesized) doped FLC W301. “As synthesized” GO may contain some undesired impurities as well as some oxygen containing functional groups in excess that could have remarkably disrupted the alignment of FLC molecules. For the mixtures with 0.1 wt. % GO-200 and GO-400 doped FLC W301, the bright and dark states are observed almost comparable to that of pure FLC W 301 (Figures 2(e)–2(h)). The different colors of the samples in bright states could have been aroused due to the fact that the cell thickness of the sample cells is not exactly the same and this slight difference in the cell thickness may cause the color change. Moreover, the ordering of the FLC molecules nearby GO flakes could have been influenced by the $\pi - \pi$ stacking interactions between the aromatic rings of GO

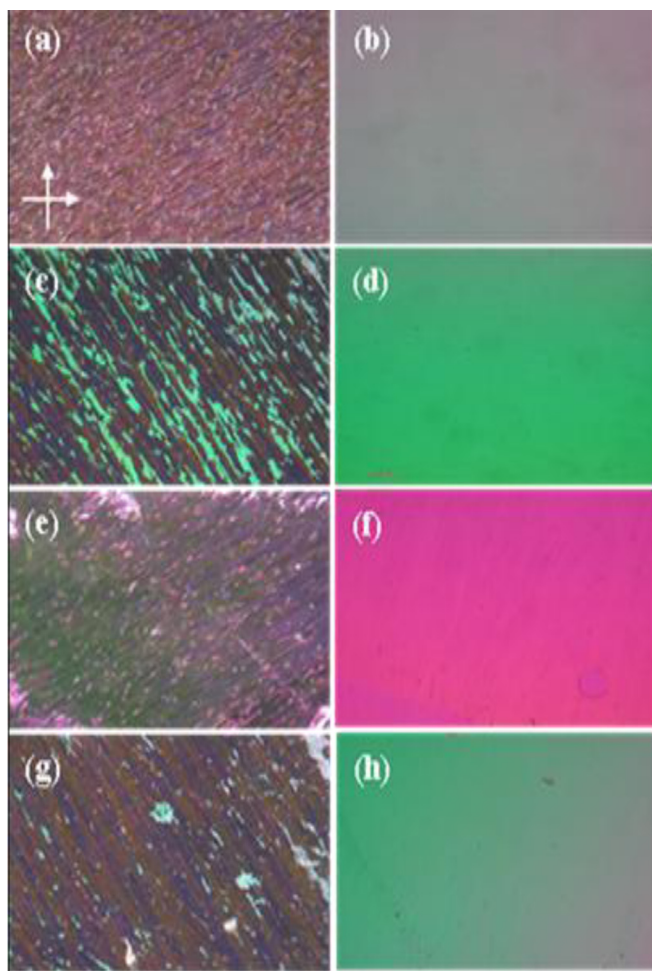


FIG. 2. Optical micrographs of dark (a), (c), (e), and (g) and bright (b), (d), (f), and (h) states of pure (a) and (b), GO doped (c) and (d), GO-200 doped (e) and (f), and GO-400 doped (g) and (h) FLC W301 at room temperature. Crossed arrows represent crossed polarizers.

flakes with that of FLC molecules.²⁹ This biased ordering of the FLC molecules nearby GO flakes has modified the local ordering which may also contribute to the phenomenon color change. The modified ordering of the FLC molecules nearby GO is shown in Figure 3.

Figure 4(a) shows the room temperature dielectric relaxation behavior of GO/FLC mixtures. It can be seen that the low frequency dielectric permittivity (ϵ') has increased by $\sim 55\%$ for as synthesized GO doped FLC. The higher values

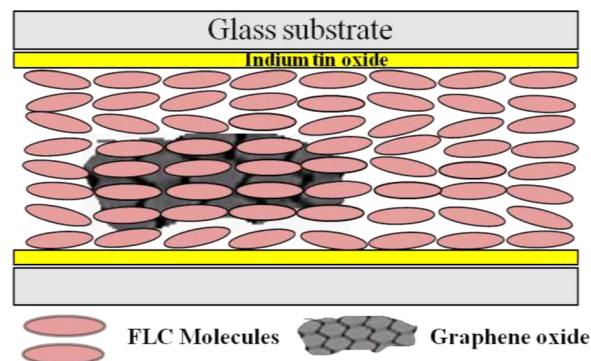


FIG. 3. The packing model showing the presence of GO flakes into the net of FLC.

of ϵ' in the case of GO doped samples could be understood by taking into account the presence of impurity ions and high polarizability of functional groups, such as $-\text{COOH}$, $-\text{OH}$, etc., attached with GO. These attached impurity ions and the functional groups contribute remarkably to ϵ' especially at low frequency regime.³⁰ Thermal treatment of GO, however, reduces such impurities and functionalities as can be seen by the value of ϵ' for thermally reduced GO doped samples.

The behavior of dielectric loss factor ($\tan \delta$) representing the different dielectric relaxation phenomena as well as energy dissipation in case of pure and GO doped samples has been shown in Figure 4(b). The peak in $\tan \delta$ around 1 kHz indicated the conventional dipolar relaxation of FLC molecules known as Goldstone mode which appear due to the phase fluctuations. The relaxation aroused at low frequency regime (~ 100 Hz) generally occurs due to the presence of undesired ionic impurities in the FLC mixture itself.^{19,31,32} Also, it may be observed that this low frequency relaxation is enhanced remarkably in case of GO doped samples and is found greater for “as synthesized” GO doped FLC sample. Such enhancement has been observed due to the presence of ionic contamination in GO and such impurities are obviously remarkable in case of “as synthesized.” Another peaking above 100 kHz is due to the ITO electrodes used in fabricating the sample cells.^{33,34} The maximum value of $\tan \delta$ of FLC W301 has been increased in the presence of GO. However, the profile of $\tan \delta$ for GO doped samples is nearly same as that pure FLC W301. The significant increase in the peak value of $\tan \delta$ is due to dipolar contributions of

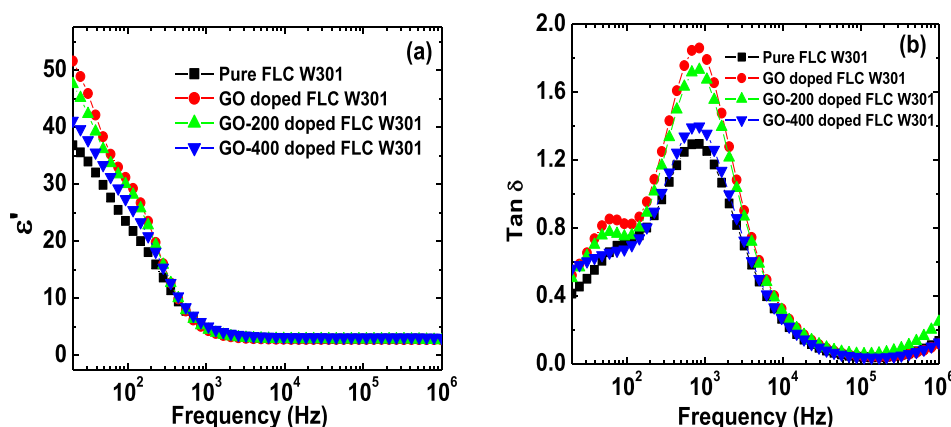


FIG. 4. Behavior of (a) dielectric permittivity (ϵ') and (b) dielectric loss factor ($\tan \delta$) of pure, GO, GO-400, and GO-400 doped FLC W301 material with frequency at room temperature.

the oxygen based functional groups attached with GO. For higher annealing temperatures, these functional groups have been reduced and in turn the ϵ' and $\tan \delta$ values became comparable to that of pure FLC W301 in case of GO-400 doped FLC. Clearly, the behavior of ϵ' and $\tan \delta$ of the GO/FLC mixtures further manifested the stepwise reduction of GO.

To analyze the interaction of GO with FLC material in terms of the material constants of the later, we observed the behavior of spontaneous polarization (P_s), rotational viscosity (η), and response time (τ_R) of GO/FLC mixtures with applied dc voltage which is shown in Figure 5. It is clear from the Figure 5(a) that the saturation value of P_s is observed almost the same for all mixtures. However, it is found to be slightly greater in case of GO doped FLC W301 especially at low bias voltages. The reasons for this increased value in P_s are due to the presence of oxygen based functional groups attached with GO. These functional groups produce polarization when field is applied and thus increasing slightly the effective value of P_s of the mixture. As the values of P_s for pure and GO doped FLC have come out to be comparable, we have averaged out all these values to get a smooth plot which is shown in the inset of Figure 5(a).

Figure 5(b) shows the change in rotational viscosity as a function of applied voltage. It is quite interesting to observe a remarkable lowering in the η values of FLC due to the presence of GO.

The rotational viscosity FLC material is found to decrease monotonically by doping with GO annealed at different (increasing) temperatures. The decrease in η may be due to the dielectric anisotropic properties of GO and FLC materials. When electric field is applied, both GO sheets and FLC molecules experience a torque but because of distinct dielectric anisotropic properties and aspect ratio, the dynamic

response is not the same which results in the reduced rotational viscosity.³⁵ The electro-optical response time (τ_R) of LC based display systems is one of the most important parameters as it provides the information about the switching speed of the device and it mainly depends on the material constants η and P_s . This dependence is given by the relation

$$\tau_R = \frac{\eta}{P_s E},$$

where E is applied field.

With the above relation, it can be clearly understood how the lowering in the rotational viscosity resulted the faster response of GO/FLC composites [Figure 5(c)]. The η values have been lowered greatly in case of GO-400 doped FLC which in turn result $\sim 20\%$ reduction in the response time.

IV. CONCLUSIONS

A systematic low temperature exfoliation and reduction of lyophilized GO has been demonstrated. The systematic thermal reduction has been performed to analyze the effect of temperature and abridging oxygen on the structure of GO sheets. By using the thermal reduction method, we have been succeeded to obtain reduced GO at comparatively lower temperature (400 °C). Furthermore, the effect of GO annealed at different temperatures on the dielectric and electro-optical properties has been analyzed. The presence of GO has lowered the rotational viscosity of FLC material which in turn resulted in the form of faster response of the GO/FLC composites. The present study is one of the steps to obtain low temperature based GO and to explore the

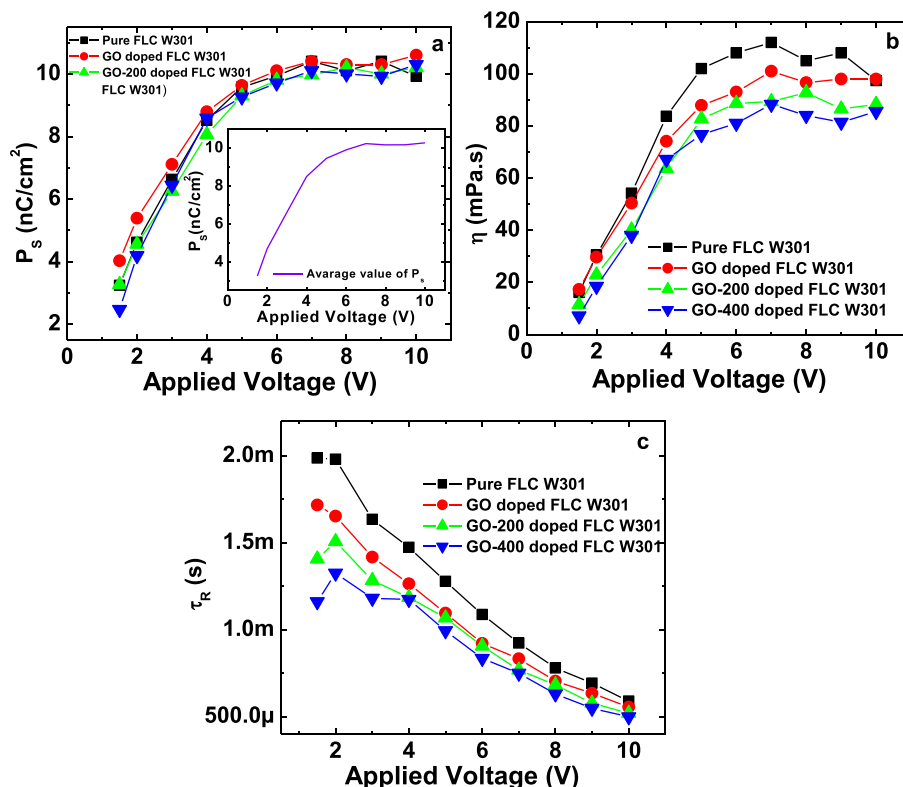


FIG. 5. Behavior of (a) spontaneous polarization (P_s), (b) rotational viscosity (η), and (c) response time (τ_R) of pure, GO, GO-200, and GO-400 doped FLC W301 material with applied voltage at room temperature. Inset of (a) shows the behavior of average value of P_s for pure and GO doped samples.

applications of the same in improving the properties of LC based display systems.

ACKNOWLEDGMENTS

Veeresh Kumar thanks University Grant Commission (UGC), Government of India for the research fellowship. The authors sincerely thank Professor R. C. Budhani, Director, CSIR-National Physical Laboratory, New Delhi for his interest in this research work. We are also thankful to Dr. S. P. Singh and Mr. A. Chandran for fruitful discussions.

- ¹A. K. Geim and K. S. Novoselov, *Nature Mater.* **6**, 183 (2007).
- ²Y. Zhu, S. Murali, W. Cai, X. Li, J. W. Suk, J. R. Potts, and R. S. Ruoff, *Adv. Mater.* **22**, 3906 (2010).
- ³F. Bonaccorso, Z. Sun, T. Hasan, and A. C. Ferrari, *Nat. Photonics* **4**, 611 (2010).
- ⁴C. N. R. Rao, A. K. Sood, K. S. Subrahmanyam, and A. Govindaraj, *Angew. Chem. Int. Ed.* **48**, 7752 (2009).
- ⁵S. Park and R. S. Ruoff, *Nat. Nanotechnol.* **4**, 217 (2009).
- ⁶O. C. Compton and S. T. Nguyen, *Small* **6**, 711 (2010).
- ⁷W. Chen, L. Yan, and P. R. Bangal, *Carbon* **48**, 1146 (2010).
- ⁸M. Acik, G. Lee, C. Mattevi, M. Chhowalla, K. Cho, and Y. J. Chabal, *Nature Mater.* **9**, 840 (2010).
- ⁹M. J. McAllister, J. L. Li, D. H. Adamson, H. C. Schniepp, A. A. Abdala, J. Liu, and I. A. Aksay, *Chem. Mater.* **19**, 4396 (2007).
- ¹⁰W. S. Hummers and R. E. Offeman, *J. Am. Chem. Soc.* **80**, 1339 (1958).
- ¹¹B. Zhao, P. Liu, Y. Jiang, D. Pan, H. Tao, J. Song, and W. Xu, *J. Power Sources* **198**, 423 (2012).
- ¹²H. C. Schniepp, J. L. Li, M. J. McAllister, H. Sai, M. Herrera-Alonso, D. H. Adamson, and I. A. Aksay, *J. Phys. Chem. B* **110**, 8535 (2006).
- ¹³L. Wan, P. Liu, T. Zhang, Y. Duan, and J. Zhang, *J. Mater. Sci.* **49**, 4989 (2014).
- ¹⁴W. Chen and L. Yan, *Nanoscale* **2**, 559 (2010).
- ¹⁵H. B. Zhang, J. W. Wang, Q. Yan, W. G. Zheng, C. Chen, and Z. Z. Yu, *J. Mater. Chem.* **21**, 5392 (2011).
- ¹⁶W. Lv, D. M. Tang, Y. B. He, C. H. You, Z. Q. Shi, X. C. Chen, and Q. H. Yang, *ACS Nano* **3**, 3730 (2009).
- ¹⁷A. Malik, A. Choudhary, P. Silotia, A. M. Biradar, V. K. Singh, and N. Kumar, *J. Appl. Phys.* **108**, 124110 (2010).
- ¹⁸V. Kumar, A. Kumar, A. M. Biradar, G. B. Reddy, D. Sachdev, and R. Pasricha, *Liq. Cryst.* **41**, 1719 (2014).
- ¹⁹A. Chandran, J. Prakash, K. K. Naik, A. K. Srivastava, R. Dabrowski, M. Czerwinski, and A. M. Biradar, *J. Mater. Chem. C* **2**, 1844 (2014).
- ²⁰S. S. Bawa, A. M. Biradar, K. Saxena, and S. Chandra, *Rev. Sci. Instrum.* **59**, 2023 (1988).
- ²¹H. Feng, R. Cheng, X. Zhao, X. Duan, and J. Li, *Nat. Commun.* **4**, 1539 (2013).
- ²²M. Acik, G. Lee, C. Mattevi, A. Pirkle, R. M. Wallace, M. Chhowalla, and Y. Chabal, *J. Phys. Chem. C* **115**, 19761 (2011).
- ²³Z. Lin, Y. Yao, Z. Li, Y. Liu, Z. Li, and C. P. Wong, *J. Phys. Chem. C* **114**, 14819 (2010).
- ²⁴A. C. Ferrari and D. M. Basko, *Nat. Nanotechnol.* **8**, 235 (2013).
- ²⁵A. C. Ferrari, J. C. Meyer, V. Scardaci, C. Casiraghi, M. Lazzeri, F. Mauri, and A. K. Geim, *Phys. Rev. Lett.* **97**, 187401 (2006).
- ²⁶H. Wang, Y. Wang, X. Cao, M. Feng, and G. Lan, *J. Raman Spectrosc.* **40**, 1791 (2009).
- ²⁷L. Kong, C. Bjelkevig, S. Gaddam, M. Zhou, Y. H. Lee, G. H. Han, and J. A. Kelber, *J. Phys. Chem. C* **114**, 21618 (2010).
- ²⁸N. A. Clark and T. P. Rieker, *Phys. Rev. A* **37**, 1053 (1988).
- ²⁹S. Y. Lu and L. C. Chien, *Opt. Express* **16**, 12777 (2008).
- ³⁰L. J. Romasanta, M. Hernández, M. A. López-Manchado, and R. Verdejo, *Nanoscale Res. Lett.* **6**, 508 (2011).
- ³¹T. Joshi, A. Kumar, J. Prakash, and A. M. Biradar, *Liq. Cryst.* **37**, 1433 (2010).
- ³²M. Y. Jin and J. J. Kim, *J. Phys.: Condens. Matter* **13**, 4435 (2001).
- ³³P. Perkowski, *Opto-Electron. Rev.* **20**, 79 (2014).
- ³⁴R. Dhar, *Ind. J. Pure Appl. Phys.* **42**, 56 (2004).
- ³⁵H. Y. Chen, W. Lee, and N. A. Clark, *Appl. Phys. Lett.* **90**, 033510 (2007).
- ³⁶See supplementary material at <http://dx.doi.org/10.1063/1.4930949> for SEM images of GO and finally reduced GO, XRD of graphite, Raman spectrum of graphite, full details of peak positions with Lorentz fitted curves.